Biochemical and Biophysical Research Communications 665 (2023) 152–158

Contents lists available at ScienceDirect

Biochemical and Biophysical Research Communications

journal homepage: www.elsevier.com/locate/ybbrc

N-carbamoyl aspartate reduced body weight by stimulating the thermogenesis of iBAT

Zhefeng Wang [a, d], Yumei Zhang [a, b, 1], Tiantian Zhou [a, d], Xin Wu [a, c, d, *]

[a] CAS Key Laboratory of Agro-ecological Processes in Subtropical Region, Institute of Subtropical Agriculture, Chinese Academy of Sciences, Changsha, Hunan, 410125, PR China
[b] State Key Laboratory of Agricultural Microbiology, Huazhong Agricultural University, Wuhan, 430070, PR China
[c] Tianjin Institute of Industrial Biotechnology, Chinese Academy of Sciences, Tianjin, 300308, PR China
[d] College of Advanced Agricultural Sciences, University of Chinese Academy of Science, Beijing, 100049, PR China

ARTICLE INFO

Article history:
Received 28 March 2023
Received in revised form
17 April 2023
Accepted 25 April 2023
Available online 4 May 2023

Keywords:
N-carbamoyl aspartate
Pyrimidine biosynthesis
Polyunsaturated fatty acid
BAT activation

ABSTRACT

Uridine has formerly been shown to alleviate obesity and hepatic lipid accumulation. N-carbamoyl aspartate (NCA) provides carbon atoms to uridine in *de novo* pyrimidine biosynthesis pathway. However, whether NCA is involved in the lipid metabolism remains elusive. Here we showed that NCA supplementation significantly decreased ($P < 0.05$) serum cholesterol (CHOL), high-density lipoprotein (HDL), lactate dehydrogenase (LDH), and alkaline phosphatase (ALP) levels of mice, and significantly increased ($P < 0.05$) relative mRNA expression of genes related to the synthesis of pyrimidine nucleotides and polyunsaturated fatty acids. Besides, supplemented with NCA significantly decreased body weight and area under the curve (AUC), and increased body temperature in the high-fat diet fed mice. For further, relative protein expression of uridine monophosphate synthase (UMPS), sterol regulatory element-binding protein 1(SREBP-1) and phosphorylated hormone-sensitive triglyceride lipase (P-HSL) in the liver, and uncoupling protein 1 (UCP-1) in interscapular brown adipose tissue (iBAT) also showed upregulated in the high-fat diet fed mice. Thus, NCA promoted *de novo* synthesis of pyrimidine and polyunsaturated fatty acid, and reduced body weight by stimulating high-fat diet-induced thermogenesis of iBAT.

1. Introduction

Obesity and overweight have become a global health issue that leads to a variety of diseases including diabetes mellitus type 2, hepatic steatosis, insulin resistance, and cardiovascular diseases [1,2]. The development of obesity is an extremely complex process, but fundamentally it occurs as a result of a chronic imbalance of energy in the body [3]. In other words, obesity develops when energy consumption less than energy intake, leading to an excess of energy storage in the form of triglycerides in white adipose tissue (WAT) [4]. Different types of adipocytes have distinct functions in the regulation of energy homeostasis [3,5,6]. WAT applies to energy storage through the synthesis and accumulation of triglycerides. In contrast, interscapular brown adipose tissue (iBAT) dissipates energy to ward off obesity by activating uncoupling protein 1 (UCP-1) in mitochondria and transforms fat through thermogenesis [3,7]. Thus preventing and remedying the obesity and its associated diseases through increasing BAT activity may be an effective therapeutic manner [4,8].

The previous study has shown that glutamine metabolism in adipose tissue is reduced in the obese state, which brings about increased nuclear O-GlcNAcylation in adipocytes, and administration of glutamine reduces adipose tissue inflammation and improves fat tissue function in obesity [9]. O-linked β-N-acetylglucosamine (O-GlcNAc) modification is controlled by a couple of intermediary metabolites including acetyl-coenzyme A, glucose, glutamine, and uridine [10]. Our recent studies have suggested that uridine can regulate hepatic pyrimidine metabolism [11,12], attenuating obesity and hepatic lipid accumulation caused by a high-fat diet [13]. N-carbamoyl aspartate (NCA) is an intermediate product of glutamine, which provides carbon atoms to uridine in *de novo* pyrimidine biosynthesis pathway [14–16]. Nevertheless, NCA has received limited attention in studies of lipid

* Corresponding author. Institute of Subtropical Agriculture, Chinese Academy of Sciences, Yuanda (Second) Road 644, Changsha, Hunan, 410125, PR China.
E-mail address: wuxin@isa.ac.cn (X. Wu).
[1] This author contributes equally.

https://doi.org/10.1016/j.bbrc.2023.04.094
0006-291X/

metabolism. Considering NCA is a precursor of uridine and is involved in glutamine metabolism, we conjectured that NCA might contribute to alleviating fat accumulation. Thus, the present study aims to investigate the effects of NCA on lipid metabolism in high-fat diet-fed mice.

2. Materials and methods

2.1. Animals and treatments

All the procedures and care standards involved in this study were performed according to the Animal Welfare Committee of the Institute of Subtropical Agriculture, Chinese Academy of Sciences (Changsha, China). Eight-week-old male C57BL/6J mice were purchased from the SLAC Laboratory Animal Central (Hunan, China) [Certificate no. SCXK (Xiang) 2019-0004]. All the mice were housed at 20 ± 2 °C, with 45 ± 5% humidity and 12 h light/dark cycle, with ad libitum access to feed and fresh water. The high-fat diet containing 65% calories purchased from BiotechHD Co., Ltd. (Beijing, China) were allowed ad libitum to feed and water.

2.2. Experimental design and sample collection

Two animal experiments were conducted. In the NCA intervention study, sixteen mice were adapted to a control diet administered free for one week, then randomly divided into two groups (n = 8): the control group (Con) received a normal chow diet and NCA group (NCA) received normal chow diet supplemented with 265.6 mg/kg/d NCA. NCA was provided by Baikang Co., Ltd (Changsha, China), dissolved in drinking water renewed every 2 days. The body weight (BW) was recorded for each week, and the experiment lasted for 4 weeks. After the end of the trial, blood was collected from the retroorbital sinus to obtain the serum sample as previously reported [17]. Hepatic tissues were collected for total RNA extraction.

In the high-fat-diet NCA intervention study, twenty-four mice were acclimated to a control chow diet administered ad libitum for one week randomly divided into two groups (n = 12): HF group (HF) received a high-fat diet (HFD) and the HF-NCA group (HF + NCA) received a high-fat diet supplemented with 265.6 mg/kg/d NCA dissolved in drinking water. The BW was recorded daily, and the feed intake was recorded weekly. The intervention lasted for 4 weeks. After completion of the experiment, mice were killed by cervical dislocation, and liver, inguinal white adipose tissue (iWAT), and iBAT tissues were immediately fixed in 4% paraformaldehyde fix solution for Oil Red O (ORO) and hematoxylin-eosin (H&E) staining, respectively. Liver and adipose tissue, including iWAT and iBAT tissues were separated and stored at −80 °C until analyzed.

2.3. Serum biochemical analysis

Serum samples were examined for glucose (GLU), total triglyceride (TG), cholesterol (CHOL), low-density lipoprotein (LDL), high-density lipoprotein (HDL), total bile acid (TBA), aspartate transaminase (AST), alanine aminotransferase (ALT), alkaline phosphatase (ALP), and lactate dehydrogenase (LDH) were analyzed by an Automated Biochemistry Analyzer (cobas c311, Roche, BSL, CH), using kits purchased from Beijing Chemlin Biotech Co., Ltd (Beijing, China).

2.4. Intraperitoneal glucose tolerance test (IPGTT)

IPGTT was performed after 12 h of fasting by intraperitoneal injection of glucose (1.5 g/kg BW). Blood samples were collected from the tail vein, and the glucose concentrations were determined at 0, 20, 40, 80, and 120 min after the injection using a One Touch Ultra Easy glucometer (Roche). The AUC was calculated.

2.5. Surface temperature measurement

The surface temperature was measured using an infrared camera (Seek Thermal Compact XR iOS Camera, Thermal).

2.6. H&E and ORO staining

For ORO staining, after being fixed with 4% paraformaldehyde for another 15 min, hepatic tissue was then put in Oil Red solution for 8–10 min in the dark, differentiation in 60% isopropanol, and immersed in hematoxylin for 3–5 min according to standard protocols.

For H&E staining, iWAT and iBAT tissues fixed with 4% paraformaldehyde were paraffin-embedded, cut in 5 μm-thick sections, then stained with H&E using standard protocols. The count and average size of adipocytes were quantified using Image J software (version 1.48r, National Institutes of Health, Bethesda, Maryland, USA).

2.7. Quantitative real-time PCR(qRT-PCR)

Total RNA was extracted from frozen liver and iBAT tissues using Trizol reagent (Invitrogen, Carlsbad, CA, USA). Then, the RNA concentration was determined using a NanoDrop ND-1000 spectrophotometer (Thermo Fisher Scientific, Wilmington, DE, USA) and cDNA was reverse transcribed using an Evo M-MLV RT Kit (Accurate Biotechnology (Hunan) Co., Ltd). The primers (Table 1) were designed and synthesized by Sangon Biotech (Shanghai) Co., Ltd. The qRT-PCRreaction was performed with SYBR Green Premix Pro Taq HS qPCR Kit (Accurate Biotechnology (Hunan) Co., Ltd) and run in a light cycler 480 II real-time PCR system (Roche, Basel, Switzerland). All procedures were coped with following the manufacturer's manual. The values of the target genes were calculated using the comparative Ct method using Actin as the housekeeping gene.

2.8. Western Blot (WB) experiment

Hepatic and iBAT tissues were lysed in RIPA buffer (Beyotime Technology, Shanghai, China) containing 1% protease inhibitor cocktail (Roche Diagnostics Corp, Pleasanton, CA, USA) followed by centrifugation at 12,000 rpm for 15 min at 4 °C. Protein content was measured using a bicinchoninic acid (BCA) assay (Beyotime Technology, Shanghai, China). Use the Wes Simple Western System (ProteinSimple, San Jose, CA, USA) for protein qualification. In detail, protein samples mixed with 0.1 × Sample Buffer, 5 × Master Mix, and Ladder were added into Wes 25-well plates. Then, primary antibodies, secondary antibodies, Antibody Diluent II, Streptavidin-HRP, Lumino-S-Peroxide mix, and Wash Buffer were added to the corresponding wells. The primary antibodies used in this experiment included UMPs (sc-135596, Santa Cruz Biotechnology), SREBP-1 (sc-365513, Santa Cruz Biotechnology), HSL (ab45422, abcam), P-HSL (ab109400, Abcam), UCP-1(U6382) (SigmaChemical Co, St. Louis, MO, USA) and GAPDH (60004-1-Ig) (Proteintech, Rosemont, IL, USA). Total protein expression was normalized to GAPDH.

2.9. Statistical analysis

The statistical analyses were assessed by the *t*-test using SPSS 22.0 (SPSS Inc., Chicago, IL, USA). All data were presented as the

Table 1
Primers used in RT-qPCR.

Gene	Accession No.	5′-3′ Primer sequence	Product Size (bp)
DHODH	NM_020046.3	F: AATACCACAGTGAGTCGCCC R: CAGATCTCGGAGTGGCTTCC	87
UMPS	NM_009471.3	F: GCAAAACGCCACGAGTTCTT R: GACTGCTGCCTTGGTGTAGT	258
CMPK2	NM_020557.4	F: CTGCTTAACTCTGCGGTGTTC R: CTTTCTGGACCTCCTTTGGGC	130
RRM2	NM_009104.2	F: CTGTTTCTATGGCTTCCAAAT R: TTCTTCTTCACACAAGGCATT	141
UPP	NM_009477.3	F: CTGACCGCTACGCCATGTAT R: AGACCTATCCCGCCTGAAGT	166
UPP2	XM_006498409.4	F: CGGTTGGAGGGAGATGGAGAA R: AATGGAAATGGAGGGGATGCC	123
FADS1	NM_146094.2	F: ACCCACCAAGAATAAAGCGCTAA R: CAGCCACATCCAGCAGCAG	134
FADS2	NM_019699.2	F: ACCGTGGCAAAAGCTCTCAG R: GAGAGGATGAACCAGGCAAGGC	151
ELOVL2	NM_001311121.1	F: AAAGGCGAAGACTGTGTGCT R: CCAGCCATATCGAGAGCAGG	277
ELOVL5	NM_134255.3	F: TGCAGCTTGCTTCTGTTCCC R: GGTACTGAGTGACGCATCGAA	134
ATGL	NM_025802.3	F: GACCTGATGACCACCCTTTC R: CAGATACTGGCAGATGCTACC	183
β-Actin	NM_007393.5	F: TGTCCACCTTCCAGCAGATGT R: AGCTCAGTAACAGTCCGCCTAGA	101

means ± standard error (SEM). There is statistically significant difference when $P < 0.05$.

3. Results

3.1. Effects of NCA on body weight, serum biochemical parameters, and the synthesis of hepatic pyrimidine nucleotides and polyunsaturated fatty acids

To investigate the impression of NCA on mice, BW and serum lipid profiles were assessed. As shown in Fig. 1A, NCA administration significantly reduced ($p < 0.05$) the serum level of CHOL, HDL, ALP, and LDH compared to the Con group (Fig. 1B–C).

To further investigate the molecular mechanism of NCA in the synthesis of hepatic pyrimidine nucleotides and polyunsaturated fatty acids, the relative mRNA expressions of genes were analyzed. Results showed that NCA treatment markedly up-regulated the relative expression of pyrimidine nucleotides synthesis genes such as dihydroorotate dehydrogenase (*DHODH*), uridine monophosphate synthase (*UMPS*), Cytidine/uridine monophosphate

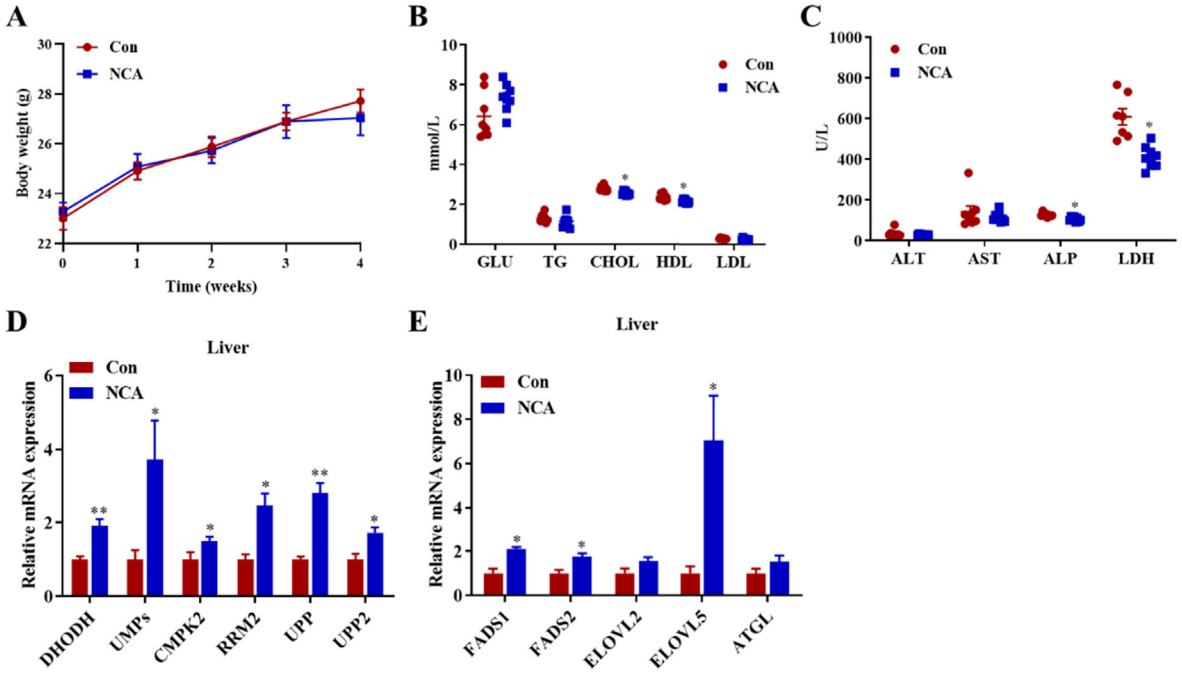

Fig. 1. Effects of NCA on body weight, serum biochemical parameters, and the synthesis of hepatic pyrimidine nucleotides and polyunsaturated fatty acids. (A) Body weight (g), (B) GLU, TG, CHOL, HDL, and LDL in serum, (C) ALT, AST, ALP, and LDH in serum, (D) Relative mRNA expression of pyrimidine biosynthesis genes in liver, (E) Relative mRNA expression of *de novo* polyunsaturated fatty acid synthesis genes in liver.

kinase 2 (*CMPK2*), ribonucleotide reductase subunit 2 (*RRM2*), uridine phosphorylase (*UPP*), and *UPP2* ($p < 0.05$) (Fig. 1D). Additionally, the gene expression of fatty acid desaturases 1 (*FADS1*), *FADS2*, and fatty acid elongase 5 (*ELOVL5*) related to the synthesis of polyunsaturated fatty acids were also increased ($p < 0.05$) in NCA-treated mice (Fig. 1E).

3.2. NCA supplementation decreased HFD-induced body weight gain (BWG), increased the core body temperature, and improved glucose tolerance

To further investigate the effect of NCA on body weight gain under a high-fat diet, 8-week-old male C57BL/6J mice were fed either HF diet or HF diet supplemented with NCA (265.6 mg/kg/day) for 4 weeks. Although NCA treatment alone did not influence the BW in mice fed a normal chow diet (Fig. 1A), it significantly prevented ($p < 0.05$) the body weight gain in HF mice (Fig. 2A). The total food intake of all the mice for the 4-week experiment was measured (Fig. 2B), showing that HF and HF + NCA mice consumed the same amount of food, inferring that NCA induced weight loss was not through reducing the food intake. Consequently, we examined whether NCA treatment could affect core body temperature by using an infrared camera. Interestingly, NCA treatment significantly enhanced ($p < 0.05$) core body temperature compared with the HF mice (Fig. 2C–D). These results evidenced that the anti-obesity role of NCA may be owing to an increase in energy expenditure. Furthermore, NCA treatment improved glucose homeostasis under HF diet (Fig. 2E–F). Results of the IPGTT, and the corresponding AUC values were a further proof that NCA supplementation significantly upgraded ($p < 0.01$) impaired glucose tolerance in HFD-fed mice.

3.3. NCA prevents liver steatosis and up-regulated the protein expression of UMPS, SREBP-1, and phosphorylated HSL

Next, histology analyses by Oil Red O staining were applied to evaluate the steatohepatitis under HFD. Mice-fed HFD showed an accumulation of lipid in the liver, which was then rescued by NCA supplementation (Fig. 3A). The effects of NCA on the pyrimidine nucleotides synthesis and fatty acid metabolism were also investigated in HFD-fed mice. As presented in Fig. 3B–E, NCA treatment up-regulated ($p < 0.05$) the protein expression of UMPS, SREBP-1, and phosphorylated HSL in HF-fed mice. These results indicated that NCA restrained the liver lipid accumulation and stimulated the synthesis of pyrimidine nucleotides, lipogenesis, and lipolysis process in HF-fed mice.

3.4. NCA stimulates BAT activation in HFD-fed mice

Finally, we tested the count and the size of adipocyte cells from iWAT and iBAT sections using Image J software. As shown in Fig. 4A–C, relative count and average adipocyte size in iWAT indicated no differences ($p < 0.05$) between groups. While the relative count of adipocyte cells in iBAT markedly increased ($p < 0.01$) after NCA treatment and the relative size of adipocyte cells was significantly decreased ($p < 0.05$) compared with the HF group (Fig. 4A, D-E). Furthermore, we measured the protein expression of thermogenic marker, UCP-1. The result showed that NCA treatment notably up-regulated ($p < 0.05$) the protein expression of UCP1 (Fig. 4A, F-G), indicating that NCA could stimulate BAT activation in HFD-fed mice.

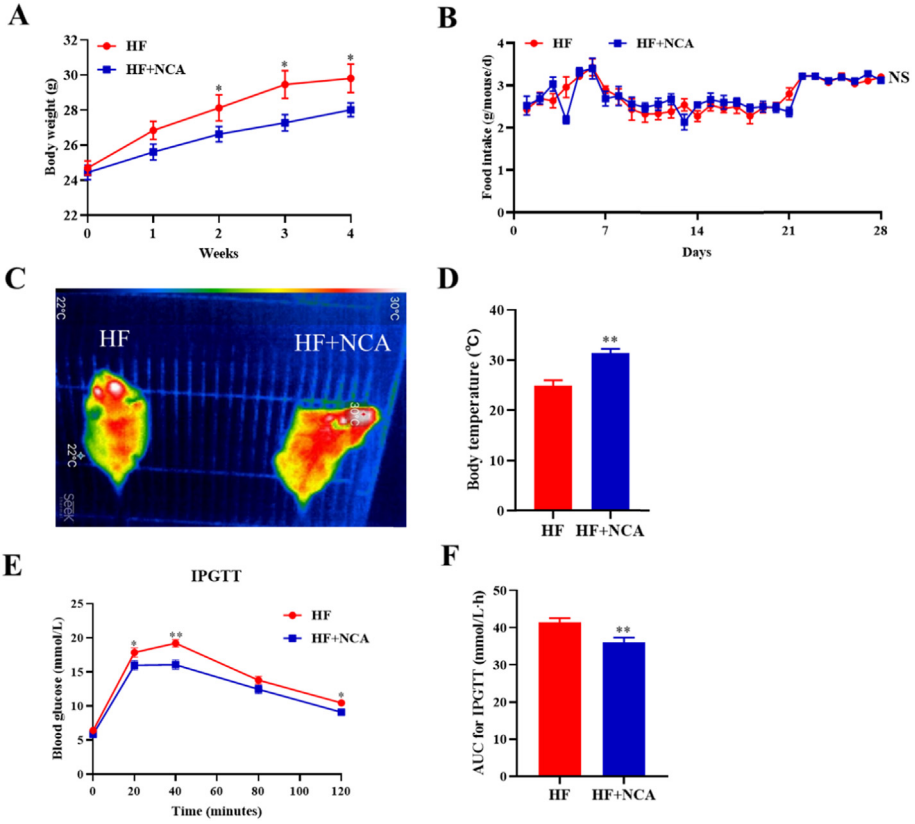

Fig. 2. NCA supplementation reduced HFD-induced body weight gain, increased the core body temperature, and improved glucose tolerance. (A) Body weight change after 4 weeks NCA treatment with HFD (n = 12), (B) Average daily food intake (n = 12), (C–D) Body temperature (n = 8), (E) IPGTT (n = 12), (F) AUC for IPGTT (n = 12).

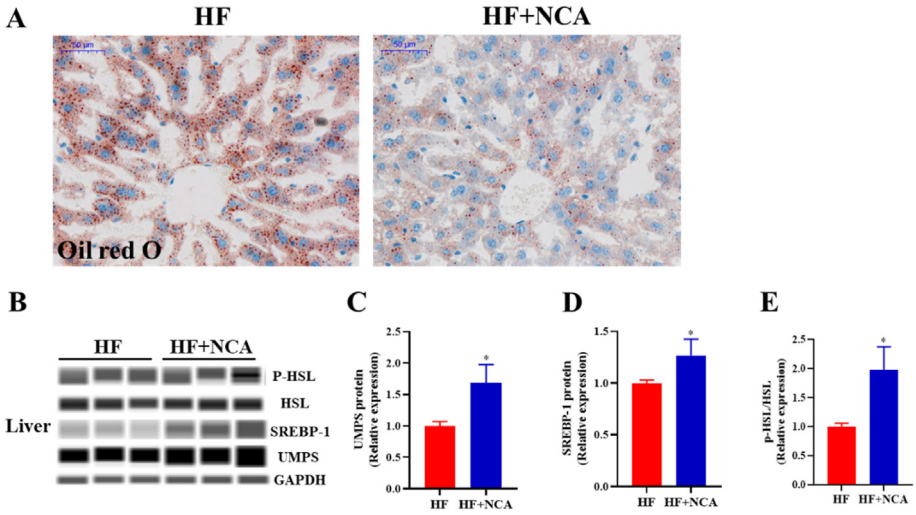

Fig. 3. NCA prevented liver steatosis and up-regulated the protein expression of UMPS, SREBP-1, and phosphorylated HSL. (A) Oil Red O staining of liver (scale bar: 50 μm), (B–E) Liver expression of UMPS, SREBP-1, and P-HSL proteins. (For interpretation of the references to colour in this figure legend, the reader is referred to the Web version of this article.)

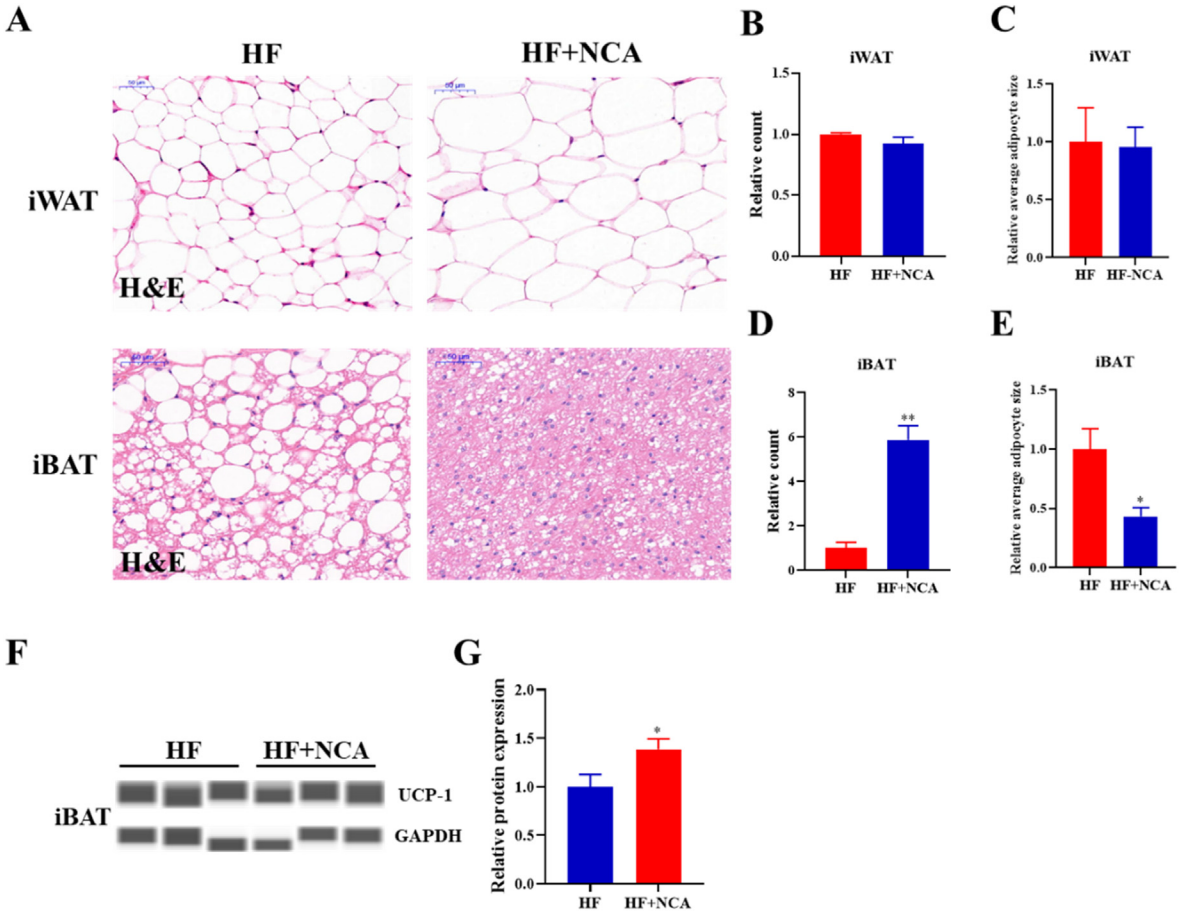

Fig. 4. NCA stimulated BAT activation in HFD-fed mice (A) H&E staining of iWAT and iBAT (scale bar: 50 μm), (B) Relative count of adipocyte cells in iWAT (n = 4), (C) Relative average adipocyte size in iWAT (n = 4), (D) Relative count of adipocyte cells in iBAT (n = 4), (E) Relative average adipocyte size in iBAT (n = 4), (F–G) Relative protein expression of UCP-1in iBAT.

4. Discussion

NCA is an intermediate metabolite of glutamine catalyzed by carbamoyl phosphate synthetase II (CPS-II) and aspartate transcarbamoylase (ATCase) [15,18]. Although acting as a precursor of uridine [18], NCA appears to be largely impermeable to cells [16]. Previous study has shown that glutamine was associated with inflammation and obesity in human white adipose tissue [9], and

uridine also lowered adipocyte area in HFD-fed mice [13]. Additionally , NCA supplementation regulated serum differential metabolites related to fatty acids metabolism. However, the effect of NCA on lipid metabolism has not been determined so far. In our research, by integrating data on serum biochemical parameters, and relative mRNA expression involved in pyrimidine biosynthesis and *de novo* synthesis of polyunsaturated fatty acid, we presented evidence that daily treatment of mice with 265.6 mg/kg/d NCA is sufficient to reduce the content of CHOL, HDL, ALP and LDH in serum, stimulates *de novo* synthesis of polyunsaturated fatty acid and pyrimidine. Furthermore, daily treatment of HFD-fed mice with NCA could prevent diet-induced body weight gain, increase the core body temperature, and improve glucose tolerance by enhancing BAT activity.

Uridine is a pyrimidine nucleotide, which is critical to maintain cellular function, energy homeostasis, and lipid metabolism [18,19]. Research indicated that uridine could prevent lipid accumulation [20], suppress hepatic droplet accumulation [21], and regulate fatty acid composition [22]. Considering that NCA is a precursor of uridine synthesis [18] and cannot penetrate the cells [16], we speculated that NCA might participate in uridine synthesis and regulate lipid metabolism, involved in lipogenesis and lipolysis. In the current study, we found the mRNA expression related to uridine metabolism was significantly increased in mice after NCA administration. Furthermore, the protein expression of UMPS in HFD-fed mice with NCA treatment also increased. UMPS is an enzyme that plays an essential role in pyrimidine synthesis, transforming orotic acid to uridine 5′ monophosphate. NCA increased the mRNA and protein expression of UMPS, indicated the role of NCA in promoting nucleotide synthesis. We previously found that dietary supplementation with uridine have no influence on serum glucose, TG, HDL, LDL, LDH, ALT, AST, and ALP levels in weaned piglets [12,23]. While we surprisingly observed different results compared to the previous studies mentioned above, in that NCA treatment significantly decrease serum CHOL, HDL, ALP, and LDH, which may suggest a beneficial effect of NCA on lipid metabolism. Further study involved in *de novo* synthesis of polyunsaturated fatty acid declared that there was a higher rate of *de novo* synthesis of polyunsaturated fatty acid in liver after NCA treatment.

Obesity is a chronic disease due to imbalanced energy metabolism induced by excessive calorie intake relative to energy consumption [24]. Uridine concentration could relate to the level of lipolysis [25]. Therefore, HFD-fed mice were used to further explore the effects of NCA on lipid metabolism. NCA treatment reduced the BW without effects on food intake in HFD-fed mice, denoting that the anti-obesity effect of NCA is unrelated to energy intake. However, the body temperature significantly enhanced after NCA treatment, suggesting that the anti-obesity effect of NCA may be attributed to increased energy expenditure, which is corresponding to the former study that showed uridine was implicated in temperature regulation and energy homeostasis [26]. NCA administration also enhanced glucose clearance consistency with an earlier research by Liu et al. [13].

Further study in the liver showed that NCA administration reduced hepatic lipids accumulation, and increased the protein expression of SREBP-1c (a regulator of fatty acid synthesis) and HSL (in charge of substrate supply for the BAT thermogenic pathway) [27]. The increased protein expression of SREBP-1c indicated that NCA stimulated hepatic fatty acid synthesis. HSL is the enzyme that provides substrates to heat and ATP production [28]. Increased HSL protein expression was shown in the NCA group, suggesting its impact on lipolysis promotion and heat production of NCA. Lower body weight gain may be due to the increases in heat production. BAT is a heat dissipation organ that adjusts insulin resistance, GLU homeostasis and facilitates a lean and healthy phenotype [29]. The significantly increased relative count and decreased average adipocyte size indicated that NCA stimulated lipolysis of iBAT. BAT can generate heat by the activation of UCP-1 [30]. The enhanced expression of UCP-1 protein in the iBAT of the HF + NCA group indicated that the decreased body weight due to NCA stimulated thermogenesis.

In conclusion, our results showed that NCA promoted *de novo* synthesis of pyrimidine and polyunsaturated fatty acid, and reduced BW by stimulating the thermogenesis of iBAT induced by HFD.

Author contributions

Xin Wu devoted to the research concept and design. Zhefeng Wang analyzed the experimental data and prepared Figures. Yumei Zhang constructed Tables and Figures and drafted the manuscript. Zhefeng Wang, Yumei Zhang, and Tiantian Zhou performed experiments, and reviewed, edited the manuscript with Xin Wu. All authors revised the manuscript and approved its submission.

Declaration of competing interest

The authors declare that they have no known competing financial interests or personal relationships that could have appeared to influence the work reported in this paper.

Acknowledgments

The research work was supported by National Natural Science Foundation of China (32272905) and Tianjin Synthetic Biotechnology Innovation Capacity Improvement Project (TSBICIP-CXRC-031; TSBICIP-CXRC-038).

References

[1] F.F. Anhe, R.T. Nachbar, T.V. Varin, J. Trottier, S. Dudonne, M. Le Barz, P. Feutry, G. Pilon, O. Barbier, Y. Desjardins, D. Roy, A. Marette, Treatment with camu camu (Myrciaria dubia) prevents obesity by altering the gut microbiota and increasing energy expenditure in diet-induced obese mice, Gut 68 (2018) 453–464, https://doi.org/10.1136/gutjnl-2017-315565.

[2] P. Xu, J. Wang, F. Hong, S. Wang, X. Jin, T. Xue, L. Jia, Y. Zhai, Melatonin prevents obesity through modulation of gut microbiota in mice, J. Pineal Res. 62 (2017), https://doi.org/10.1111/jpi.12399.

[3] Y. Xu, N. Wang, H.Y. Tan, S. Li, C. Zhang, Z. Zhang, Y. Feng, Panax notoginseng saponins modulate the gut microbiota to promote thermogenesis and beige adipocyte reconstruction via leptin-mediated AMPKalpha/STAT3 signaling in diet-induced obesity, Theranostics 10 (2020) 11302–11323, https://doi.org/10.7150/thno.47746.

[4] L.H. Quan, C. Zhang, M. Dong, J. Jiang, H. Xu, C. Yan, X. Liu, H. Zhou, H. Zhang, L. Chen, F.L. Zhong, Z.B. Luo, S.M. Lam, G. Shui, D. Li, W. Jin, Myristoleic acid produced by enterococci reduces obesity through brown adipose tissue activation, Gut 69 (2019) 1239–1247, https://doi.org/10.1136/gutjnl-2019-319114.

[5] A. Graja, S. Gohlke, T.J. Schulz, Aging of Brown and beige/brite adipose tissue, Handb. Exp. Pharmacol. 251 (2019) 55–72, https://doi.org/10.1007/164_2018_151.

[6] B. Li, L. Li, M. Li, S.M. Lam, G. Wang, Y. Wu, H. Zhang, C. Niu, X. Zhang, X. Liu, C. Hambly, W. Jin, G. Shui, J.R. Speakman, Microbiota depletion impairs thermogenesis of Brown adipose tissue and browning of white adipose tissue, Cell Rep. 26 (2019) 2720–2737 e2725, https://doi.org/10.1016/j.celrep.2019.02.015.

[7] E.P. Mottillo, E.M. Desjardins, J.D. Crane, B.K. Smith, A.E. Green, S. Ducommun, T.I. Henriksen, I.A. Rebalka, A. Razi, K. Sakamoto, C. Scheele, B.E. Kemp, T.J. Hawke, J. Ortega, J.G. Granneman, G.R. Steinberg, Lack of adipocyte AMPK exacerbates insulin resistance and hepatic steatosis through Brown and beige adipose tissue function, Cell Metabol. 24 (2016) 118–129, https://doi.org/10.1016/j.cmet.2016.06.006.

[8] M. Zietak, P. Kovatcheva-Datchary, L.H. Markiewicz, M. Stahlman, L.P. Kozak, F. Backhed, Altered microbiota contributes to reduced diet-induced obesity upon cold exposure, Cell Metabol. 23 (2016) 1216–1223, https://doi.org/10.1016/j.cmet.2016.05.001.

[9] P. Petrus, S. Lecoutre, L. Dollet, C. Wiel, A. Sulen, H. Gao, B. Tavira, J. Laurencikiene, O. Rooyackers, A. Checa, I. Douagi, C.E. Wheelock, P. Arner, M. McCarthy, M.O. Bergo, L. Edgar, R.P. Choudhury, M. Aouadi, A. Krook,

M. Ryden, Glutamine links obesity to inflammation in human white adipose tissue, Cell Metabol. 31 (2019) 375–390, https://doi.org/10.1016/j.cmet.2019.11.019.
[10] J.P. Etchegaray, R. Mostoslavsky, Interplay between metabolism and epigenetics: a nuclear adaptation to environmental changes, Mol. Cell 62 (2016) 695–711, https://doi.org/10.1016/j.molcel.2016.05.029.
[11] Y. Liu, Y. Zhang, J. Yin, Z. Ruan, X. Wu, Y. Yin, Uridine dynamic administration affects circadian variations in lipid metabolisms in the liver of high-fat-diet-fed mice, Chronobiol. Int. 36 (2019) 1258–1267, https://doi.org/10.1080/07420528.2019.1637347.
[12] Y. Zhang, S. Guo, C. Xie, R. Wang, Y. Zhang, X. Zhou, X. Wu, Short-Term oral UMP/UR administration regulates lipid metabolism in early-weaned piglets, Animals (2019) 9, https://doi.org/10.3390/ani9090610.
[13] Y. Liu, C. Xie, Z. Zhai, Z.Y. Deng, H.R. De Jonge, X. Wu, Z. Ruan, Uridine attenuates obesity, ameliorates hepatic lipid accumulation and modifies the gut microbiota composition in mice fed with a high-fat diet, Food Funct. 12 (2021) 1829–1840, https://doi.org/10.1039/d0fo02533j.
[14] A.N. Lane, T.W. Fan, Regulation of mammalian nucleotide metabolism and biosynthesis, Nucleic Acids Res. 43 (2015) 2466–2485, https://doi.org/10.1093/nar/gkv047.
[15] J.L. Liu, May the force Be with you: metabolism of arginine and pyrimidines, J. Genet. Genomics 42 (2015) 179–180, https://doi.org/10.1016/j.jgg.2015.05.003.
[16] C. Mao, X. Liu, Y. Zhang, G. Lei, Y. Yan, H. Lee, P. Koppula, S. Wu, L. Zhuang, B. Fang, M.V. Poyurovsky, K. Olszewski, B. Gan, DHODH-mediated ferroptosis defence is a targetable vulnerability in cancer, Nature 593 (2021) 586–590, https://doi.org/10.1038/s41586-021-03539-7.
[17] X. Zhou, L. He, S. Zuo, Y. Zhang, D. Wan, C. Long, P. Huang, X. Wu, C. Wu, G. Liu, Y. Yin, Serine prevented high-fat diet-induced oxidative stress by activating AMPK and epigenetically modulating the expression of glutathione synthesis-related genes, Biochim. Biophys. Acta, Mol. Basis Dis. 1864 (2018) 488–498, https://doi.org/10.1016/j.bbadis.2017.11.009.
[18] L.M. Gao, G.Y. Liu, H.L. Wang, T. Wassie, X. Wu, Y.L. Yin, Impact of dietary supplementation with N-carbamoyl-aspartic acid on serum metabolites and intestinal microflora of sows, J. Sci. Food Agric. 103 (2023) 750–763, https://doi.org/10.1002/jsfa.12186.
[19] Y. Deng, Z.V. Wang, R. Gordillo, Y. An, C. Zhang, Q. Liang, J. Yoshino, K.M. Cautivo, J. De Brabander, J.K. Elmquist, J.D. Horton, J.A. Hill, S. Klein, P.E. Scherer, An adipo-biliary-uridine axis that regulates energy homeostasis, Science (2017) 355. https://doi.org/10.1126/science.aaf5375.
[20] T.T. Le, A. Ziemba, Y. Urasaki, E. Hayes, S. Brotman, G. Pizzorno, Disruption of uridine homeostasis links liver pyrimidine metabolism to lipid accumulation, J. Lipid Res. 54 (2013) 1044–1057, https://doi.org/10.1194/jlr.M034249.
[21] T.T. Le, Y. Urasaki, G. Pizzorno, Uridine prevents tamoxifen-induced liver lipid droplet accumulation, Bmc Pharmacol. Toxicol. 15 (2014), https://doi.org/10.1186/2050-6511-15-27.
[22] L.M. Gao, Y.L. Liu, X. Zhou, Y. Zhang, X. Wu, Y.L. Yin, Maternal supplementation with uridine influences fatty acid and amino acid constituents of offspring in a sow-piglet model, The Br. J. Nutr. 125 (2021) 743–756. https://doi.org/10.1017/s0007114520003165.
[23] C.Y. Xie, Q. Wang, G. Li, Z. Fan, H. Wang, X. Wu, Dietary supplement with nucleotides in the form of uridine monophosphate or uridine stimulate intestinal development and promote nucleotide transport in weaned piglets, J. Sci. Food Agric. (2019), https://doi.org/10.1002/jsfa.9850.
[24] Y. Li, Z. Ma, S. Jiang, W. Hu, T. Li, S. Di, D. Wang, Y. Yang, A global perspective on FOXO1 in lipid metabolism and lipid-related diseases, Prog. Lipid Res. 66 (2017) 42–49, https://doi.org/10.1016/j.plipres.2017.04.002.
[25] Y. Deng, Z.V. Wang, R. Gordillo, Y. Zhu, A. Ali, C. Zhang, X. Wang, M. Shao, Z. Zhang, P. Iyengar, R.K. Gupta, J.D. Horton, J.A. Hill, P.E. Scherer, Adipocyte Xbp1s overexpression drives uridine production and reduces obesity, Mol. Metabol. 11 (2018) 1–17, https://doi.org/10.1016/j.molmet.2018.02.013.
[26] Y. Deng, Z.V. Wang, R. Gordillo, Y. An, C. Zhang, Q. Liang, J. Yoshino, K.M. Cautivo, J. De Brabander, J.K. Elmquist, An adipo-biliary-uridine axis that regulates energy homeostasis, Science 355 (2017), https://doi.org/10.1126/science.aaf5375 eaaf5375.
[27] C.A.P. de Souza, C.C. Gallo, L.S. de Camargo, P.V.V. de Carvalho, I.F. Olescuck, F. Macedo, F.M. da Cunha, J. Cipolla-Neto, F.G. do Amaral, Melatonin multiple effects on brown adipose tissue molecular machinery, J. Pineal Res. 66 (2019), https://doi.org/10.1111/jpi.12549.
[28] H. Sell, Y. Deshaies, D. Richard, The brown adipocyte: update on its metabolic role, Int. J. Biochem. Cell Biol. 36 (2004) 2098–2104, https://doi.org/10.1016/j.biocel.2004.04.003.
[29] K.I. Stanford, R.J. Middelbeek, K.L. Townsend, D. An, E.B. Nygaard, K.M. Hitchcox, K.R. Markan, K. Nakano, M.F. Hirshman, Y.H. Tseng, L.J. Goodyear, Brown adipose tissue regulates glucose homeostasis and insulin sensitivity, J. Clin. Invest. 123 (2013) 215–223, https://doi.org/10.1172/JCI62308.
[30] P.P. Argentato, H. de Cassia Cesar, D. Estadella, L.P. Pisani, Programming mediated by fatty acids affects uncoupling protein 1 (UCP-1) in brown adipose tissue, Br. J. Nutr. 120 (2018) 619–627, https://doi.org/10.1017/S0007114518001629.